Structural Investigation of Solid-Acid-Promoted Pd/SDB Catalysts for Ethyl Acetate Production from Ethanol

J.-F. Lee,[†] F.-S. Zheng,[‡] and J.-R. Chang*[,‡]

Department of Chemical Engineering, National, Chung Cheng University, Chia-Yi, Taiwan, R. O. C., and Synchrotron Radiation Research Center, Hsinchu, Taiwan, R. O. C.

Received: September 13, 2000; In Final Form: January 9, 2001

Catalyzed by styrene-divinylbenzene copolymer (SDB)-supported Pd (Pd/SDB) catalysts, ethyl acetate can be formed from water-containing ethanol via concomitant partial oxidation and esterification reaction. The partial oxidation reaction is carried out over palladium clusters on the catalysts. The esterification reaction is catalyzed by protons formed from the spontaneous dissociation of acetic acid and can be enhanced by addition of solid acid catalysts. To investigate the nature of solid acid in promoting the catalytic properties of Pd/SDB catalysts, extended X-ray absorption fine structure (EXAFS) and inductively coupled plasma optical emission (ICP) spectroscopy were used to characterize the reaction-induced morphology change of Pd clusters and metal loss. After the reaction, there is no evidence of palladium oxide formation, suggesting that the oxidation reaction takes place via the adsorbed oxygen. In addition, concomitantly with Pd leaching, increase of average Pd cluster size was observed. Pd−Pd coordination number increases from 3.0 to 7.9 and the Pd content decreases from 1.0 to 0.55 wt %. Addition of acid catalysts reduces leaching and growth of Pd clusters. This effect increases with an increase in acid-to-Pd catalyst ratio of the mixed catalysts. As the acid-to-Pd catalyst ratio increases from 1.0 to 4.0, Pd−Pd coordination number decreases from 7.2 to 6.5 and the Pd content increases from 0.63 to 0.71 wt %.

Introduction

In conversion of water-containing ethanol to ethyl acetate catalyzed by conventional hydrophilic catalysts such as Pd/γ-Al_2O_3, the water film formed in capillary condensation could cover the palladium clusters. The water film not only impedes the forward chemical reaction but also retards the diffusion of reactants to actives sites.[1] Because of the strong mass-transfer limitation; hydrophilic Pd catalysts present a relatively lower reaction rate than that catalyzed by hydrophobic styrene-divinylbenzene copolymer (SDB)-supported Pd catalysts. However, the hydrophobic catalysts deactivates rather fast because of the loss of Pd metal and the decrease of Pd dispersion during the reaction.[1,2]

The metal loss results from leaching of palladium(II) acetate via the reaction between palladium clusters and acetic acid.[1] Since smaller clusters are leached preferentially in the process, the dispersion of the Pd catalysts would thus be decreased. However, the decrease of dispersion may also be caused by Pd agglomeration. The works of Zhang et al., Anderson et al., and Chang et al., indicate that the interactions between adsorbates and metal clusters may weaken the metal−support interactions, resulting in a migration and agglomeration of metal clusters.[3−5]

Although oxylchlorination is normally used for reactivation of a supported metal catalyst by the redispersion of aggregated metal clusters, it has not been applied in industry for SDB-supported Pd catalysts.[6] Besides, the activity loss caused by metal leaching is not recoverable. Because of these two shortcomings, the industrial application of Pd/SDB catalysts in ethyl acetate production is difficult.

Acetic acid is formed from the oxidation of ethanol catalyzed by Pd clusters. It can be further catalytically esterified to ethyl acetate by the dissociated protons. However, acetic acid dissociation is limited by a thermodynamic equilibrium and is not enough for efficient catalytic esterification. To increase the acidity of the catalyst system so as to decrease acetic acid formation, resin-type solid acid catalysts were added to the Pd/SDB catalysts. The change of yield pattern caused by the addition of the acid catalysts might affect Pd−adsorbate interactions, leading to a change in morphology of Pd clusters and the consequent catalytic properties of Pd/SDB. Extended X-ray absorption fine structure (EXAFS) technique has been shown to be useful for quantitative characterization of the structure of supported metal catalysts.[7−11] It will also allow us to investigate the nature of active sites for ethanol partial oxidation. Moreover, the correlation of catalyst structure with catalytic performance test results will help us to investigate the role of acid catalysts in enhancing the catalytic properties of the Pd catalysts. The results would point to a way for further improving the catalyst performance.

Experimental Section

Material and Catalyst Preparation. The SDB support with a BET surface area of 465 m^2/g was prepared by polymerizing divinylbenzene in ethylvinylbenzene with 2,2-azobis(2-methylpropionitrile) as initiator. The Pd/SDB catalysts were prepared by impregnating the SDB with an ethanol solution containing a given amount of $Pd(NH_3)_4Cl_2 \cdot H_2O$. The amounts were chosen so that adsorption of all the Pd precursors would yield a solid containing 1.0 wt % Pd. The details of the preparation method have been reported in a paper by Yaparpalvi and Chung.[12]

The resin-type solid acid catalysts used in this study are sulfonic acid ion-exchange resins, Amberlyst 35 (Rohm Haas).

* Corresponding author. Tel: 886-5-2720411, ext 6239. E-mail: chmjrc@ccunix.ccu.edu.tw.
[†] Synchrotron Radiation Research Center.
[‡] Chung Cheng University.

10.1021/jp0032457 CCC: $20.00
Published on Web 04/06/2001

Catalytic Performance. The catalytic performance tests were carried out in a continuous downflow fixed-bed reactor with an inside diameter of 2.1 cm and volume of 94.0 mL. The reactor was heated with a water-bath circulator, and the reaction temperature was monitored with a sensor in the center of the catalyst bed. Two grams of Pd/SDB catalysts was mixed with a certain amount of resin-type catalysts to give an acid-to-Pd catalyst ratio of 1.0 and 4.0 by weight, respectively. The mixed catalysts were diluted with 1.6 mm glass balls to a total catalyst bed of about 50 mL. A gradient packing method was used to minimize bypassing effects. Before the test the catalyst was reduced in H_2 at 150 °C for 8 h. The reaction then was carried out with a weight hourly space velocity (WHSV) of 2.4 h^{-1} (g of feed/h·g of catalyst), at 95 °C, 35.4 atm, and a air/ethanol molar ratio = 2.37. The reaction products were trapped by a condenser at −5 °C and analyzed using a gas chromatograph (Shimadzu gas chromatograph model GC-14B; TCD and FID detector, equipped with a DB-WAX capillary column, 30 m long; and a SP4270 data processor). The metal leached was analyzed using inductively coupled plasma optical emission spectroscopy with a Jarnell-Ash 1100 instrument.

X-ray Absorption Spectroscopy. The X-ray absorption measurements were performed on X-ray beamline X-11 of the National Synchrotron Light Source (NSLS) at Brookhaven National Laboratory with a storage ring energy of 2.5 GeV and a beam current between 150 and 250 mA. A Si(111) double-crystal monochromator was used for energy selection, and it was detuned 20% at $E_0 + 50$ eV to suppress higher harmonic radiation; resolution, $\Delta E/E$, was estimated to be 2.0×10^{-4}. The monochromator was scanned in the energy range from 200 eV below to 1200 eV above the palladium K absorption edge (24 350 eV) edge. The catalyst samples were pressed into a self-supporting wafer with the wafer thickness chosen to give an absorbance of 2.5 and reduced at the same operation conditions as those for the catalytic performance tests. The EXAFS measurements were performed in the transmission mode at liquid nitrogen temperature. The transmission measurement geometry was arranged using gas-filled ionization chambers to monitor the intensities of the incident and transmitted X-rays. To gain the proper absorption ratio for the incoming X-rays, the gas compositions in the ionization chamber were selected at an argon to nitrogen mole ratio of 1/1 for the first chamber and pure argon for the second chamber, respectively. X-ray absorption data from three scans of each sample were averaged, and then the preedge and background were subtracted. Each resulting spectrum was divided by the edge height to obtain EXAFS functions.[13]

Results and Discussion

Role of the Acid Catalyst in Ethanol Conversion and Metal Loss. Similar to the reaction catalyzed by Pd/SDB catalysts, the conversion of ethanol catalyzed by the mixed catalysts increased with reaction time to about 25 h on stream and then declined. At about 70 h on stream, the change of catalytic properties as well as the leaching of Pd became insignificant.[1] The catalytic performance of the Pd/SDB catalysts and the mixed catalysts was then examined by comparing ethanol conversion, product selectivity, and Pd loss. The results are summarized in Table 1. As expected, ethanol conversion increased with acid-to-Pd catalyst ratio, while metal loss decreased because of the increase of esterification reaction.

In a previous paper, we reported that Pd is leached out in the reaction system as measured by ICP optical emission spectroscopy. The Pd leaching rate decreased with time on stream.[1] As the smaller clusters were selectively leached, the Pd leaching rate decreased and became rather slow after 70 h on stream. The leached species has been identified as palladium(II) acetate, which was formed from reaction of Pd clusters with the reaction intermediate, acetic acid. The decrease in metal loss with increasing acid catalysts suggests that the addition of acid catalyst promotes the esterification reaction, resulting in a decrease of acetic acid concentration and succeeding palladium(II) acetate formation, thereby reducing Pd leaching.

TABLE 1: Summary of Catalytic Properties and Metal Loss for Pd/SDB and Solid Acid Promoted Pd/SDB Catalysts[a]

	2 g Pd/SDB	2 g Pd/SDB + 2 g Amberlyst 35	2 g Pd/SDB + 8 g Amberlyst 35
ethanol conversion, mol %	44.3	51.4	55.5
selectivity to ethyl acetate, %	54.6	70.2	77.0
selectivity to acetic acid, %	38.0	23.2	18.0
selectivity to acetaldehyde, %	1.5	1.8	2.0
selectivity to fuel gas, %	5.9	4.8	3.0
Pd loss during reaction, %	45.2	37.0	29.0

[a] Catalysts were lined out in the reaction system for 70 h.

Role of the Acid Catalyst in Product Selectivity. Addition of acid catalysts enhanced the conversion of acetic acid to ethyl acetate. As the acid catalyst was added to form a mixed catalyst with a acid-to-Pd catalyst ratio of 4, the selectivity for ethyl acetate increased from 55 to 77%, while the selectivity for acetic acid decreased from 38 to 18% (Table 1). In this study, the selectivity to ethyl acetate [(ethyl acetate yield/ethanol conversion) 100%] has a relative standard deviation (RSD) of about 2%, caused by the deviation of gas chromatography measurement.

Fuel gas, shown in Table 1, includes methane, ethylene, CO_2, and a trace of ethylene. CO_2 is formed from the total oxidation reaction and the cracking of oxygen-containing compounds, methane from the cracking reaction, and ethylene from the dehydration reaction. Fuel gas formation decreased with increasing acid-to-Pd catalyst ratio, which might be a consequence of increasing coke formation catalyzed by acid catalyst. Coke deposited on the Pd sites might retard total oxidation and metal cracking and thus reduced fuel gas formation. Coke deposition might also reduce the adsorption of oxygen on Pd clusters, leading to a slight increase of acetaldehyde formation.

Morphology of Pd Clusters on the Fresh and the Used Pd/SDB Catalysts. The EXAFS data were analyzed using experimentally determined reference files obtained from standard materials of known structure. The Pd−Pd and Pd−O contributions were analyzed with phase shifts and backscattering amplitudes extracted from EXAFS data for palladium foil and palladium oxide, respectively, and the Ru−C contribution from EXAFS data for $Ru_3(CO)_{12}$. The appropriateness of using the Ru−C to represent Pd−C is justified by the theoretical calculation of Teo and Lee.[14] Their results show that the amplitude and phase function of the nearest and next-nearest neighbors in the periodic table are hardly different.

The comparisons of EXAFS spectra for the four samples are shown in Figure 1. The raw EXAFS data for the samples have a signal-to-noise ratio >40 (The noise amplitude was determined at $k = 14$ Å^{-1}, and signal amplitude was determined at $k = 4$ Å^{-1}).

The Fourier transforms provide the qualitative information about the morphology of the Pd clusters on the SDB support. k^3-weighted Pd−Pd phase- and amplitude-corrected Fourier transforms were performed for the EXAFS functions ($4.5 < k < 14.0$ Å) to investigate the morphology difference of Pd clusters among the fresh catalysts and the used catalysts of different acid-to-Pd-catalysts ratio.

TABLE 2: EXAFS Results[a,b]

shell	N	R, Å	$\Delta\sigma^2$	ΔE_0, eV	EXAFS ref
		a. Fresh Pd/SDB Catalyst			
Pd−$C_{support}$	2.2 ± 0.2	2.01 ± 0.01	0.002 ± 0.001	6 ± 2	Ru−C
Pd−Pd	3.0 ± 0.2	2.741 ± 0.003	−0.0003 ± 0.0004	**−2.5 ± 0.4**	Pd−Pd
		b. Used Pd/SDB Catalyst			
Pd−$O_{support}$	0.25 ± 0.05	2.16 ± 0.02	−0.009 ± 0.002	13 ± 4	Pd−O
Pd−Pd	7.9 ± 0.1	2.755 ± 0.001	−0.0016 ± 0.0001	1.3 ± 0.1	Pd−Pd
		c. Used Pd/SDB Catalyst Promoted by Acid Catalysts with Acid-to-Pd Ratio of 1.0			
Pd−$O_{support}$	0.23 ± 0.03	2.16 ± 0.01	−0.010 ± 0.001	6 ± 3	Pd−O
Pd−Pd	7.2 ± 0.1	2.760 ± 0.001	−0.0020 ± 0.0001	1.1 ± 0.1	Pd−Pd
		d. Used Pd/SDB Catalyst Promoted by Acid Catalysts with Acid-to-Pd Ratio of 4.0			
Pd−$O_{support}$	0.19 ± 0.05	2.13 ± 0.02	−0.010 ± 0.002	12 ± 5	Pd−O
Pd−Pd	6.6 ± 0.1	2.745 ± 0.001	−0.0029 ± 0.0001	0.8 ± 0.1	Pd−Pd

[a] Z is the atomic number; N the coordination number for the absorber-backscatterer pair; R the average absorber-backscatterer distance; $\Delta\sigma^2$ the Debye−Waller factor, and ΔE_0 the inner potential correction. [b] The number of parameters used to fit the data in this first shell is 8; the statistically justified number is estimated from the Nyquist theorem, $n = (2\Delta k\Delta r/\pi) + 1$, where Δk and Δr, respectively, are the k and r ranges used in the forward and inverse Fourier transform.

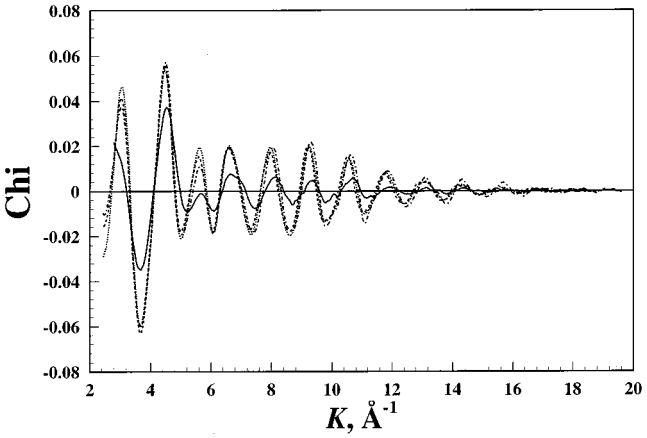

Figure 1. Raw EXAFS data for the fresh Pd/SDB catalyst (solid line), the used Pd/SDB catalyst (dashed−dotted line), the used Pd/SDB catalyst promoted by solid acid catalysts with acid-to-Pd catalyst ratio of 1.0 (dashed line), and the used Pd/SDB catalyst promoted by solid acid catalysts with an acid-to-Pd catalyst ratio of 4.0 (dotted line).

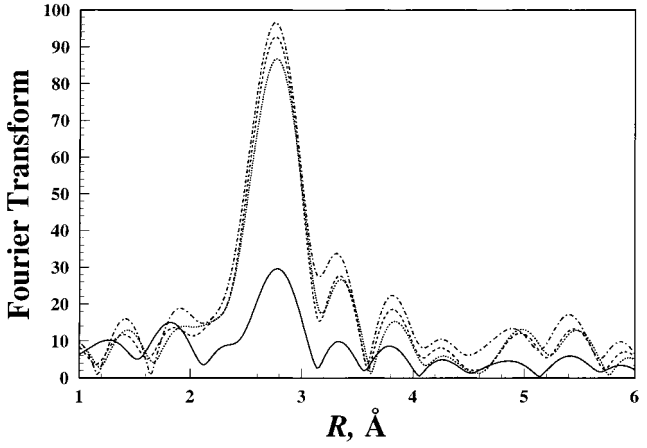

Figure 2. Magnitude of Fourier transform (k^3-weighted, $\Delta k = 4.5-14.0$ Å^{-1}, Pd−Pd phase and amplitude corrected) of the raw EXAFS data for the fresh Pd/SDB catalyst (solid line), the used Pd/SDB catalyst (dashed−dotted line), the used Pd/SDB catalyst promoted by solid acid catalysts with acid-to-Pd catalyst ratio of 1.0 (dashed line), and the used Pd/SDB catalyst promoted by solid acid catalysts with acid-to-Pd catalyst ratio of 4.0 (dotted line).

As shown in Figure 2, the Pd−Pd phase- and amplitude-corrected Fourier-transformed EXAFS functions of all the samples show that the peaks corresponding to the first metal−metal shell (at about 2.7 Å) and higher shells (about 3.8, 4.8, and 5.6 Å) are at the same positions and consistent with the nearest four neighbors in bulk fcc (face centered cubic) Pd, while the intensities of the Fourier-transformed EXAFS functions for the three used catalysts are much higher than those of the fresh catalysts and decreased with increasing acid-to-Pd catalyst ratio. Since the intensity is proportional to coordination number of Pd−Pd,[7] the decrease of the intensity with increasing acid-to-Pd catalyst ratio (Figure 2) indicates that the reaction-induced Pd agglomeration was impeded by the addition of acid catalysts.

Selective oxidation can be catalyzed by bulk metal oxide, a core of metal covered by a shell of metal oxide, or oxygen-activated metal.[16,17] The possibility of bulk metal oxide being active sites for the oxidation was rule out on the basis of the EXAFS spectra characterizing the used catalysts; bulk fcc Pd clusters were characterized, indicating that no significant contribution from bulk metal oxide was apparent and it consequently could not be the active site.

Since the residual spectrum obtained from the subtraction of Pd−Pd contributions from raw EXAFS data represented the metal−support interactions, metal−adsorbate interactions, or the metal oxide shell, further discrimination of the characteristics of active sites could be obtained from the residual spectrum.

Detailed EXAFS Analysis and Metal−Adsorbate Interactions. A k^2-weighted Fourier transformation without correction was performed on the EXAFS function over the range $4.09 < k < 14.88$ Å^{-1} for the fresh catalyst sample and $3.34 < k < 15.31$ Å^{-1} for the used one. The major contributions were isolated by inverse Fourier transformation of the data in the range $1.11 < r < 3.14$ Å for the fresh catalyst sample and $1.35 < r < 3.17$ Å for the used catalyst samples. The Fourier-filtered EXAFS data were analyzed by a difference files techniques with a nonlinear least-squares multiple-shell fitting routine.[15] The resulting coordination parameters and the corresponding standard deviations are summarized in Table 2. The number of parameters used to fit the data in this main-shell analysis is 8; the statistically justified number, calculated from the Nyquist theorem, is 14.[9]

For an X−Y absorber−backscattering pair, peaks that have a positive imaginary part of the phase-corrected EXAFS function are due to neighbors of atom type Y.[18] For the fresh catalyst, the Ru−C phase-corrected Fourier transformation of the residual spectrum of raw EXAFS data minus Pd−Pd contributions shows a positive peak at 2.0 Å (Figure 3), suggesting interactions between palladium clusters and SDB supports; carbon in SDB is the backscattering atom.

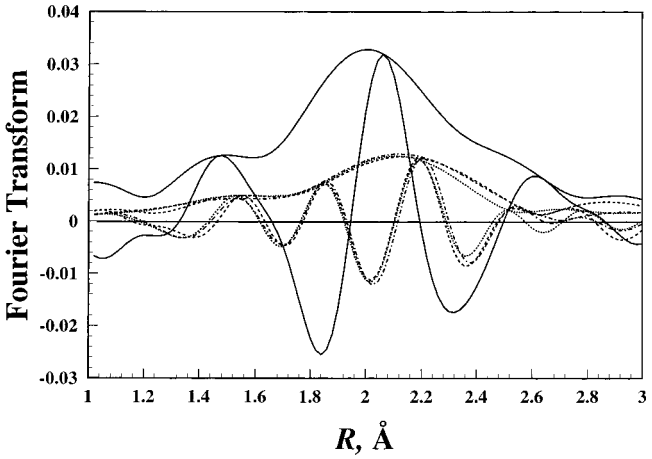

Figure 3. Fourier transform (k^1-weighted, Ru−C phase corrected for the fresh catalyst and Pd−O phase corrected for used catalysts, $\Delta k = 4.5-10.0$ Å^{-1}) for original filtered EXAFS data minus the calculated Pd−Pd EXAFS: the fresh Pd/SDB catalyst (solid line), the used Pd/SDB catalyst (dashed−dotted line), the used Pd/SDB catalyst promoted by solid acid catalysts with acid-to-Pd catalyst ratio of 1.0 (dashed line), and the used Pd/SDB catalyst promoted by solid acid catalysts with acid-to-Pd catalyst ratio of 4.0 (dotted line).

For the used Pd/SDB samples, the magnitude of Pd−O phase-corrected Fourier transformation of the residual spectra extend down to about 1.8 Å. The positive peak of the imaginary part in the envelope appeared at about 2.2 Å (Figure 3) and was assigned to contribution from the interactions between palladium clusters and oxygen. Another peak appeared at about 1.85 Å, which might be contributed from metal−support interactions, Pd−C. However, since the Pd−C and Pd−O spectra in Figure 3 practically overlap and the peak of Pt−C decreases with reaction-induced Pd agglomeration, only the main contribution, Pd−O, of the spectra was analyzed.

The Pd−O contribution is about 0.15 Å longer than the bond distance of palladium oxide. The possibility of a core of metal covered by a shell of metal oxide might thus be ruled out. Hence, we suggested that chemisorbed oxygen-containing Pd clusters provide the active sites for the oxidation reaction. The reaction mechanism is consistent with selective ethylene oxidation on supported silver catalysts.[16,19]

The Pd−O contribution might also be assigned as the contribution from the interactions between Pd clusters and the carboxyl group of acetic acid. The assignment was consistent with the leaching of Pd clusters via the formation of palladium(II) acetate and the agglomeration of Pd clusters. At the initial stage of palladium(II) acetate formation, the interactions between Pd clusters and acetic acid may weaken metal−support interactions, leading to a mobile Pd cluster. The mobile Pd cluster may either form palladium(II) acetate and be extracted from the support or migrate to strongly bound Pd clusters on the support and attach to them. Since smaller clusters are leached easily, this process concomitantly leaches out small Pd cluster from catalysts and transfers to bigger one.

Since the affinity of Pd for the organic species in the reaction system might be greater than that for SDB support, those organic species might bond to Pd clusters more strongly and loosen the interaction between Pd clusters with support. After the formation of organo-Pd complex, the complex might be leached and then reacted with acetic acid to form palladium(II) acetate. In addition, it might migrate on the SDB surface and then coalesced to form a bigger cluster.

We have attempted to add acid catalyst to Pd catalysts to minimize formation of acetic acid, thereby relieving the leaching and aggregating of Pd during the reaction. As expected, the reaction intermediate, acetic acid, was decreased by the catalytic esterification reaction and the selective oxidation reaction was increased by the abatement of metal loss and metal agglomeration (Table 1). However, because the esterification reaction is limited by a thermodynamic equilibrium, the presence of acetic acid in a significant amount is inevitable. The presence of a high level of acetic acid leads to corrosion of the equipment and damage to the catalyst. To overcome this problem, several azeotropic distillation columns with recycle as well as catalytic distillation should be used, leading to a complicated and expensive operation. A relatively cheap and simple method to overcome the thermodynamic limitation in the esterification reaction is to develop a catalyst with a different affinity for each reaction species. On the basis of the experimental results in this study, dual function catalysts with poor affinity for ethyl acetate relative to other polar species, mainly water, ethanol, and acetic acid, were developed.[20] By use of the catalyst, esterification is catalyzed by the acidic component of the catalyst and takes place mainly on the catalyst surface. Thus, a thermodynamic equilibrium among the reaction mixture can be reached on the catalyst surface. Since ethyl acetate desorbed faster than other species, it was selectively and continuously removed from the reacting surface to overcome the thermodynamic equilibrium limitation. The reduction in acetic acid concentration in the system also minimized the leaching and aggregating of Pd metal.

Conclusions

On the basis of EXAFS spectroscopy characterizing the fresh and used Pd/SDB catalyst, we suggested that chemisorbed oxygen on Pd metal is the active species in selective oxidation of ethanol to acetic acid. Part of the acetic acid was further catalytically converted to ethyl acetate by the proton dissociated from acetic acid. However, because of the deterioration of the catalysts caused by leaching and the aggregation of Pd clusters during reaction, it is difficult to develop an industrial process for ethyl acetate production using Pd/SDB catalysts. The drawbacks of the catalysts were alleviated by mixing resin-type solid acid catalyst with Pd/SDB to enhance the acidity of the catalyst system. ICP and EXAFS spectroscopy characterizing the used catalysts indicated that the leaching and aggregation of Pd clusters were decreased with increasing acid-to-Pd catalyst ratio. Performance tests suggest that the improvement in catalytic properties was mainly due to the reduction of acetic acid resulting from esterification catalyzed by the acid catalysts. The alleviation of the interaction between acetic acid and metal clusters reduces palladium(II) acetate formation, thereby decreasing the transportation of relatively mobile small clusters to form big clusters. As a result, both ethanol conversion and selectivity to ethyl acetate were increased.

Acknowledgment. The EXAFS data were analyzed using the XDAP Data Analysis Program, developed by M. Vaarkamp, J. C. Linders, and D. C. Koningsberger, and the reference files were provided by Dr. B. C. Gates. This research was supported by the National Science Council of the Republic of China (Contract No. NSC 88-2214-E-194-004). We are grateful to the staff of beam line X-11A at the National Synchrotron Light Source for their assistance.

References and Notes

(1) Lin, T.-B.; Chung, D.-L.; Chang, J.-R. *Ind. Eng. Chem. Res.* **1999**, *38*, 1275.

(2) Lin, T.-B.; Chuang, K. T.; Tsai, K.-Y.; Chang, J.-R. Process for Ethyl Acetate Production, U.S. Patent 5,770,761, 1998.

(3) Zhang, Z.; Chen, H.; Sheu, L.-L.; Sachtler, W. M. H. *J. Catal*. **1991**, *127*, 213.

(4) Anderson, S. L.; Mizushima, T.; Udagawa, Y. *J. Phys. Chem.* **1991**, *95*, 6603.

(5) Chang, J.-R.; Koningsberger, D. C.; Gates, B. C. *J. Am. Chem. Soc*. **1992**, *97*, 4196.

(6) Fung, S. C. CHEMTECH **1994**, *Jan*, 40.

(7) Kampers, F. W. H. *EXAFS in Catalysis: Instrumentation and Application*; Ph.D. Dissertation, Eindhoven University of Technology, The Netherlands, 1988.

(8) Vaarkamp, M. *The Structure and catalytic Poperties of Supported Platinum Catalysts*; Ph.D. Dissertation, Utrecht University, The Netherlands, 1993.

(9) Koningsberger, D. C.; Prins, R. *X-ray Absorption; Principles, Applications, Techniques of EXAFS, SEXAFS, and XANES.* John Wiley & Sons: New York, 1988.

(10) Gates, B. C. *Catalytic Chemistry* John Wiley & Sons: New York, 1992.

(11) Thomas, J. M.; Thomas, W. J. *Heterogeneous Catalysis* VCH Publishers Inc., New York, 1997.

(12) Yaparpalvi, R.; Chuang, K. T. *Ind. Eng. Chem. Res.* **1991**, *30*, 2219.

(13) van Zon J. B. A. D. *Extended X-ray Absorption Fine Structure Spectroscopy Design of a Spectrometer and Application to Rhodium Supported on Alumina Catalysts.* Ph.D. Dissertation, Eindhoven University of Technology, The Netherlands, 1988.

(14) Teo, B.-K.; Lee, P. A. *J. Am. Chem. Soc*. **1979**, *101*, 11, 2819.

(15) Varrkamp, M. *XDAP User's Guide.* XAFS Services International, 1996.

(16) Marcinkowsky, A. E.; Berty, J. M. J. *Catal*. **1973**, *29*, 494.

(17) Oyama, S. T.; Hightower, J. W. *Catalytic Selective Oxidation* American Chemical Society, Washington, DC, 1993.

(18) Lee, P. A.; Beni, G. *Phys. Rev.* **1977**, *B15*, 2862.

(19) Kenson, R. E. *J. Phys. Chem*. **1970**, *74*, 1493.

(20) Yan, T.-Y.; Chang, J.-R. Process for Production of Aliphatic Ester, U.S. patent in application, serial number 09/559339, 2000.